Impedans
PLASMA MEASUREMENT

Ion energy and angular distributions measured in a planar Ar/O$_2$ ICP using the Semion RFEA system

INTRODUCTION

In this study the authors compare calculated IEDs from a hybrid model with measured IEDs from the Impedans' Semion System (retarding field energy analyser) as a function of bias powers and oxygen content.

Inductively coupled plasmas (ICPs) produce high plasma density at low discharge pressure which is why they are frequently employed in semiconductor manufacturing processes. The efficiency and anisotropy of the etching process is determined by the ion flux, ion energy and ion angle. In order to manipulate them independently, it is vital to apply a radio frequency (RF) bias power to the wafer electrode. In this inductive/capacitive hybrid discharge, the ICP power controls the ion flux, while the RF bias power controls the ion energy and angular distributions (IEDs and IADs).

Although a lot of studies on IEDs under various discharge conditions have been done both experimentally and numerically in order to improve the quality of the etching process, there still exist some unanswered questions. Therefore, to fill the gaps, a hybrid model has been developed to systematically investigate IEDs and IADs in Ar/O$_2$ discharges for various ICP powers, pressures, bias powers, bias frequencies and gas ratios. A Semion System retarding field energy analyser is used to validate the plasma model. The results obtained in this work give more insight into the dependency of IEDs and IADs on the discharge parameters. which is of great importance for the
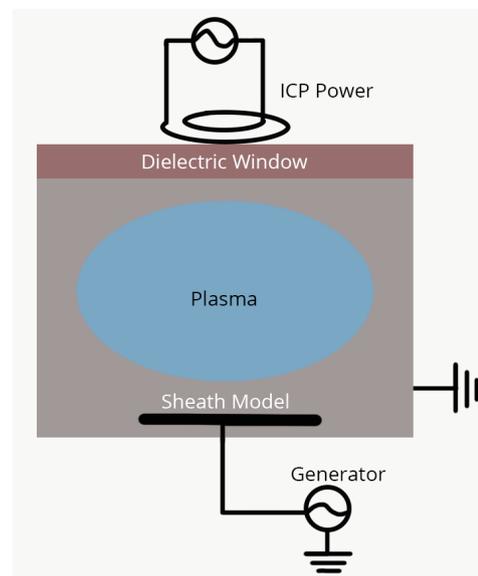

Figure 1. Schematic diagram of the ICP reactor.

improvement of etching rate and etch anisotropy.

EXPERIMENT

The schematic diagram of the ICP reactor used throughout this study is shown in figure 1. The chamber radius and height are 15.0 cm and 14.0 cm, respectively. The biased electrode has a radius of 12.2 cm, and it is placed 10.4 cm away from the quartz window, which has a dielectric constant of 7.5. A two-turn planar coil, with inner and outer radii of 6.5 cm and 9.0 cm, is placed above the dielectric window to drive the discharge. In fact, only half of the reactor axial section is modeled to improve the computational efficiency. The hybrid
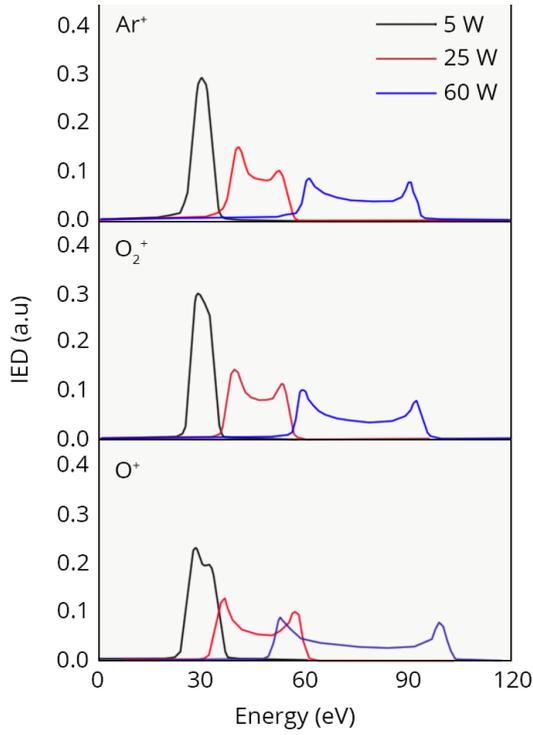
Figure 2. Ion Energy Distribution (model) of Ar^+, O_2^+ and O^+ ions Vs bias power.

Figure 3. Ion Energy Distribution (model) of Ar^+, O_2^+ and O^+ ions Vs bias frequency.

model comprises of:

(a) Fluid Model

(b) Sheath Model

(c) Ion Monte Carlo Model

The IEDs and IADs on the RF biased electrode are investigated as a function of bias powers, bias frequencies, gas ratios, ICP powers and pressure in Ar/O_2 mixtures.

RESULTS

A. Ion Energy Distribution

The low and high energy peaks of the IEDs move to higher energy with increasing bias power and O_2 content. Whereas, an opposite tendency is observed with an increase of either the ICP power or discharge pressure. In figure 2, the influence of bias power on IEDs of Ar^+, O_2^+ and O^+ is illustrated in Ar/O_2 (0.8/0.2) mixtures at 20 mTorr at the ICP power of 300 W and the bias frequency of 13.56 MHz. At low bias power (5 W), IEDs of Ar^+ and O_2^+ have a single peak, while the IED of O^+ shows a bimodal distribution. As the bias power increases, IEDs of Ar^+ and O_2^+ ions shift from unimodal to bimodal distributiobns,
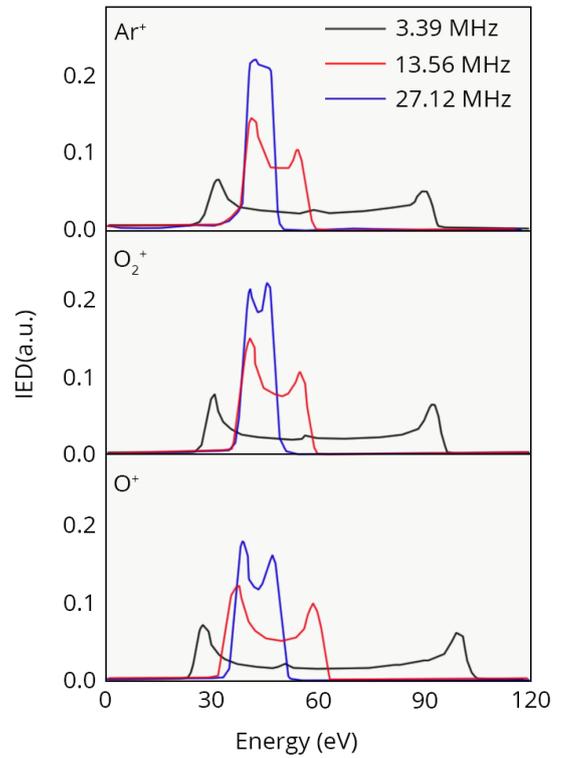
due to shorter transit time because of the larger sheath potential drop. In addition, the ion energy peaks move to higher values with increasing bias power, and the ion energy separation becomes wider. The effects of bias frequency on IEDs of Ar^+, O_2^+ and O^+ when the bias power is fixed at 25 W is shown in figure 3. Ar^+ ions respond to the transient sheath potential drop, and this gives rise to the bimodal ion energy distribution. As the bias frequency decreases, the IED peak splitting increases. The gas ratio also has a significant influence on the etching process.

The gas ratio effect on IEDs has been investigated in this work, as shown in figure 4. For $Ar:O_2 = 9:1$, the peaks of the IED of Ar^+ appear at 38.3 eV and 50.3 eV, respectively. As the concentration of O_2 increases, both the low energy peak and the high energy peak move to higher energy. This could be attributed to the longer transit time due to the thicker sheath at larger O_2 content.

When the O_2 fraction increases from 10% to 50%, the maximum sheath thickness increases from 0.095 cm to 0.157 cm, and this implies that ions could obtain more energy when they accelerate across the sheath. The variation of IEDs of O_2^+ and O^+ with O_2 content is similar to that of Ar^+,
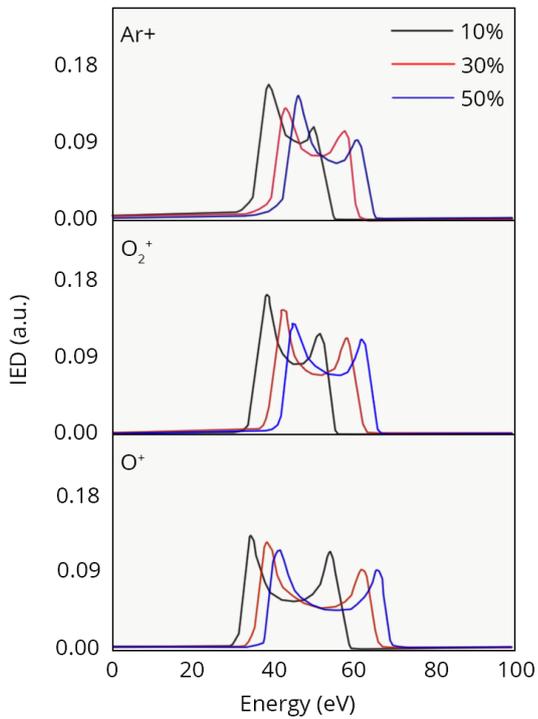
Figure 4. Ion Energy Distribution (model) of Ar^+, O_2^+ and O^+ vs O_2 at ICP Power.

Figure 5. Ion Energy Distribution (model) of Ar^+, O_2^+ and O^+ Vs pressure at ICP Power 300 W.

except for wider ion energy separation due to different ion masses. It can be seen from the figure 5 that as the pressure increases, the peaks of IEDs move to lower energy, which agrees well with those measured by a quadrupole mass spectrometer together with a cylindrical mirror energy analyser in O_2 discharges. It is noted that when the pressure increases from 10 mTorr to 30 mTorr, the minimum of the sheath potential drop (which contributes to the low energy peak) decreases, and this results in the shift of the low energy peak towards lower energy. Although the maximum of the sheath potential drop (which determines the position of the high energy peak) increases slightly with pressure, indicating that the ions could gain more energy from the stronger electric field in the sheath, the energy absorption is significantly limited at 30 mTorr due to the intensive collisions between ions and atoms or molecules. Since the energy loss of the ions rather than the energy absorption plays a dominant role, the high energy peak also shifts to lower energy.

B. Ion Angular Distribution

Another crucial factor for plasma processing is the IAD arriving at the substrate, which affects the etching efficiency and anisotropy. It is therefore important 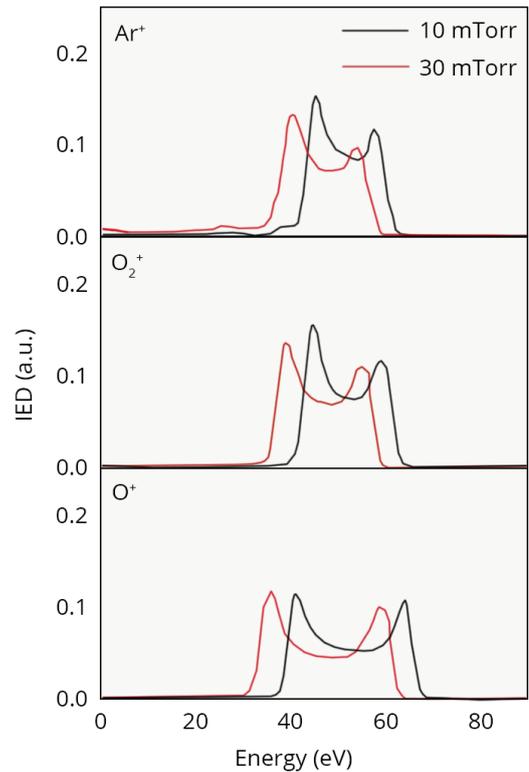to investigate the changes in IADs with discharge parameters. The proportion of incident ions with a smaller deflection angle becomes larger with increasing bias power. This is attributed to the stronger electric field in the sheath due to the increased sheath potential drop at higher bias powers. Thus, the ions bombard the electrode with higher perpendicular velocity, and this leads to a smaller deflection angle. It is clear that IAD becomes wider as the bias frequency increases, due to the weaker electric field caused by the decrease of the sheath potential drop, as we mentioned above.

The influence of O_2 content on IADs of Ar^+, O_2^+ and O^+ is displayed in figure 6. It is noted that more ions are incident on the electrode with a smaller angle as O_2 content increases. This is because the larger sheath potential drop in the wider sheath gives rise to the higher ion energy and perpendicular velocity. Therefore, a better anisotropy is achieved for larger O_2 concentrations. The peak value of IADs decreases with increasing pressure, indicating that the proportion of ions perpendicularly incident on the electrode declines. This is because the collison probability of ions when the pressure becomes higher, due to the higher density of neutral particles, resulting in a larger scattering angle.
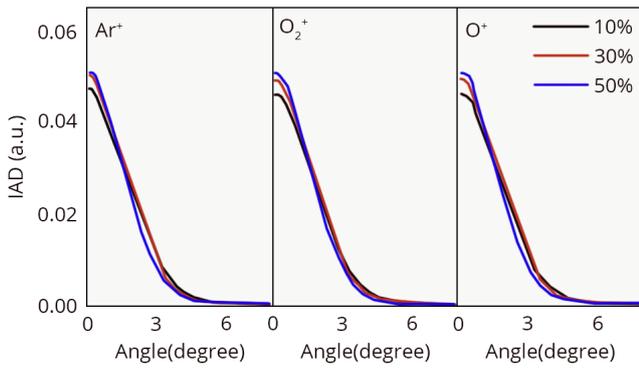
Figure 6. Ion Angular Distribution (model) of Ar^+, O_2^+ and O^+ Vs O_2 content at ICP Power 300 W.

The ICP power has a negligible influence on IADs (not shown here), except that the peak value of IADs becomes slightly lower with ICP power.

Clearly, a larger percentage of ions incident on the electrode have a smaller deflection angle as a function of increasing bias power or decreasing pressure, and a similar evolution is observed with the decrease of bias frequency. Better collimation of ions is obtained at larger O_2 concentration, but ICP power has little influence on the IADs.

C. Comparison of IED and IAD

The inductive power is delivered to the reactor through a matching network to drive the discharge. A two-turn planar coil is placed above the quartz window on the top of the vacuum chamber with water cooling inside. The substrate electrode is driven with a separate RF bias power source and is located 10.4 cm below the quartz window. The stainless cylindrical chamber is grounded and Ar/O_2 mixtures are introduced to the ICP chamber, with a total gas flow of 50 sccm. The RFEA is placed at the center of the substrate to measure IEDs.

When the bias power increases to 60 W, the two peaks shift towards higher energy, because the ions gain more energy from the stronger electric field in the sheath. The simulated IEDs show a similar behavior, except the positions of the low and high energy peaks. For instance, the two peaks appear at 54.4 eV and 78.5 eV at 50 W. his difference is caused by the fact that in the experiment, bias power is delivered to the electrode through a matching network, which means it cannot be fully coupled into the discharge. As a result, the actual power absorbed by the plasma,
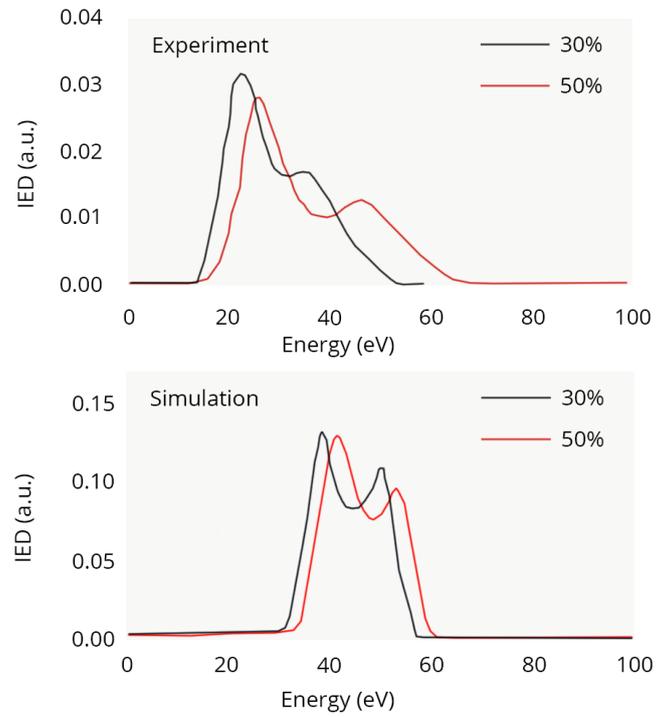

Figure 7. Comparisons of IEDs (experiment and simulation) for different O_2 contents.

as well as the sheath potential drop, is lower than in the simulation. Therefore, the peaks of simulated IEDs appear at higher energy, and the ion energy separation width in the simulation is larger.

The comparison under various O_2 contents is shown in figure 7. As O_2 fraction increases, both the measured and calculated bimodal structures move to higher energy due to the thicker sheath, as we mentioned above. Similar to the comparison for various bias powers, the peaks in the experiment appear at lower energy than in the simulation, again due to the power transfer efficiency.

CONCLUSION

Good agreement has been achieved between the simulation results of IEDs with those measured by a retarding ion energy analyser. The results obtained in this work provide a more fundamental understanding of the influence of the different discharge parameters on the IEDs and IADs, which could be used to guide and improve the etching process.

REFERENCES:

* Yu-Ru Zhang et al, "Ion energy and angular distributions in planar Ar/O$_2$ inductively coupled plasmas: hybrid simulation and experimental validation."

Journal of Physics D: Applied Physics.

Doi: 10.1088/1361-6463

Published in 2019.

* Yu-Ru Zhang et al, "Ion energy and angular distributions in planar Ar/O$_2$ inductively coupled plasmas: hybrid simulation and experimental validation."